Multifunctional Hybrid Module for Manipulators

Canberk Sozer, Sujit Kumar Sahu, Linda Paterno and
Arianna Menciassi

May 31, 2022

Multifunctional hybrid module for manipulators

Canberk Sozer[1], Sujit Kumar Sahu[2,3,4], Linda Paterno[2,3], Arianna Menciassi[2,3]

[1]Department of Automatic Control and Systems Engineering, The University of Sheffield, UK

[2]The BioRobotics Institute, Scuola Superiore Sant'Anna Pisa, Italy

[3]Department of Excellence in Robotics & AI, Scuola Superiore Sant'Anna Pisa, Italy

[4]ICube, CNRS, University of Strasbourg, INSA Strasbourg, Strasbourg, France

c.sozer@sheffield.ac.uk

INTRODUCTION

The modularity concept in manipulators relies on connecting multiple elementary structures to achieve more complex and functional systems [1]. It has promising advantages, such as affordability and higher robustness [2], and allows for better adaptability to changing needs, e.g. enlarging the system workspace. Thus, modularity is highly desired in soft robotics applications, from minimally invasive surgery [3] to deep-sea exploration [4].

In this context, the hybrid soft-rigid approach is an effective method that combines different materials to allow for the main benefits of soft (i.e., compliance and a high degree of freedom) and rigid (i.e., force generation and precision) structures [5].

This study proposes a novel hybrid soft-rigid module that combines actuation in 3D space, proprioceptive sensing, and controllable variable stiffness. The general-purpose module has major advantages, such as compactness, lightweight, low-cost, and easy fabrication using a conventional 3D printer. The design and experimental characterization are here reported. The serial integration of three modules is finally shown.

MATERIALS AND METHODS

The overview of the module is given in Fig. 1a. The module is a compact and low-cost solution that combines actuation in 3D space, variable stiffness - both controlled by air pressure -, and proprioceptive sensing. The module is 17 mm in outer diameter with a 3 mm working channel at the centre and 35 mm in length. The weight of the module is 7 g, and the material cost is less than €3 per module.

The module consists of rigid parts (VisiJet M3 Crystal, 3D Systems, USA), rigid yet compliant springs (751-663, RS PRO, UK), soft chambers (Ecoflex 00-50, Smooth-On, USA), and soft stiffness pads (Dragon Skin 10 Medium, Smooth-On, USA) (Fig. 1b).

For actuation, three spring-reinforced soft actuators are equally placed around the module with a 120° distribution, providing the motion ability in 3D space. Each actuator consists of a soft cylindrical pressure chamber and a spring. Upon pressurization of an actuator, the spring limits the radial expansion of the soft chamber but allows for elongation. Thanks to the rigid ball joint as a rotation centre, the elongation of the actuators allows for omnidirectional bending of the module up to 30° (Fig. 1c). The total bending angle can be increased by integrating multiple modules serially.

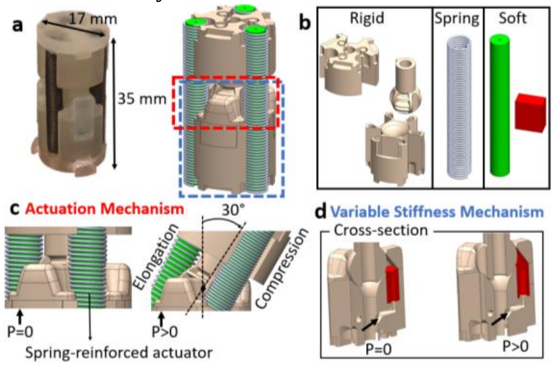

Fig. 1 (a) Overview of the module; **(b)** module components; **(c)** actuation and **(d)** variable stiffness mechanisms.

The spring as a reinforcement element did not only limit the radial expansion of the pressurized soft actuator but also behaved like an inductive sensor for proprioceptive sensing at the same time. The change in the length due to elongation and compression changes the inductance of the spring. The relationship between induced voltage, current, and the geometrical properties of the sensor can be written as follows:

$$V_L = \frac{\mu n^2 A}{l} \frac{dI_L}{dt} \qquad (1)$$

where V_L is the induced voltage, μ, n, A, l are core permeability, number of turns, cross-sectional area, and length of the spring, respectively, and $\frac{dI_L}{dt}$ is the rate of current change through the sensor. Eq. (1) shows that the induced voltage is inversely correlated with the length of the sensor. Therefore, it is expected that while the induced voltage of the sensor of the pressurized actuator decreases due to the elongation, the induced voltage of the other two sensors increases due to the compression. Thus, by measuring the voltage of three sensors simultaneously, the bending angle and direction of the module can be estimated.

For variable stiffness, three stiffness pads were placed into the dedicated slots in the bottom rigid part. Upon pressurization (Fig. 1d), the top membrane of the stiffness pads expands toward the ball joint, and the increased friction between the membrane and joint surface reduces the motion ability of the joint, thus resulting in stiffness enhancement of the module. This approach allowed for tuning the stiffness of the module without position dependency. The bottom rigid part has been designed to pressurize three pads simultaneously to increase the uniformity of the applied force to the ball joint at the centre. The pressure is distributed to the three pads through a structural airway within the rigid structure. Therefore, one inflation tube is enough to control the stiffness of the entire module.

RESULTS

Fig. 2a shows the relationship between applied pressure and bending angle of the module when one actuator is pressurized up to 200 kPa. The module reaches 30° at 120 kPa pressure. Although the pressure continues to increase up to 200 kPa, the bending angles remain the same due to the rigid structure design. The maximum standard deviations for 5 trials were calculated as ±4.4° at around 10°, where the friction between rigid parts is maximum. Indeed, the actuators were installed to the rigid structure with pre-elongation. Although this enabled to keep the rigid parts together, increased the friction in between.

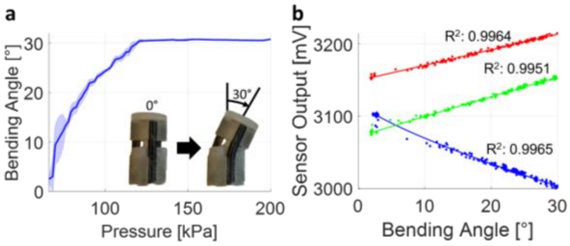

Fig. 2 Relationship between **(a)** the applied pressure - bending angle and **(b)** the bending angle – induced voltage at the three sensors (given with R^2 errors to the fitted power curve). Blue colour represents the pressurized actuator. Red and green colours indicate passively compressed actuators.

Fig. 2b demonstrates the induced voltage change at the three springs while one actuator is pressurized to bend the module up to 30°. Manual fabrication of the actuators and their instalment inaccuracies to the rigid structure caused variations (i.e., 3153, 3104, and 3076 mV) when they are in the same length at 0° straight position. According to the power curve fitting to 5 trials, the induced voltage at the elongated actuator decreases (100 mV) while the induced voltage at the passively compressed other two actuators increases (80 and 61 mV), thus providing sufficient change to be correlated with the bending angle and bending direction of the module.

Fig. 3 presents the controllable variable stiffness capability of the module. For this experiment, stiffness pads were pressurized up to 500 kPa with 100 kPa intervals when the module was fixed at 0°. Then, a force sensor was pushed toward the module for 3 mm and the force was recorded. Finally, the recorded last force value was divided by the displacement (i.e., 3 mm). According to the average of 5 trials, upon pressurization, the stiffness of the module can be increased by up to 95% (from 0.12 to 0.23 N/mm) in a controllable way.

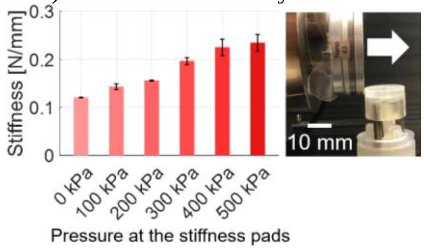

Fig. 3 Experimental result of the relationship between pressure at the stiffness pads and the stiffness of the module.

DISCUSSION

The study reports the design and experimental characterization of a module that is compact, low-cost, lightweight, and easy to fabricate using a conventional 3D printer.

The module that combines actuation in 3D space, proprioceptive sensing, and controllable variable stiffness is proposed as a general-purpose technology. Therefore, it can be adapted to use in a wide range of applications. For example, a multifunctional endoscope can be built by integrating multiple modules for steering a biopsy forceps in the tortuous shape of the colon. As shown in Fig. 4a, both single and double curvature can be achieved by tuning the actuation and variable stiffness structure, properly. Alternatively, an ultrasound tool can be attached to the tip of the endoscope (Fig 4b) to deliver non-invasive ultrasound therapy.

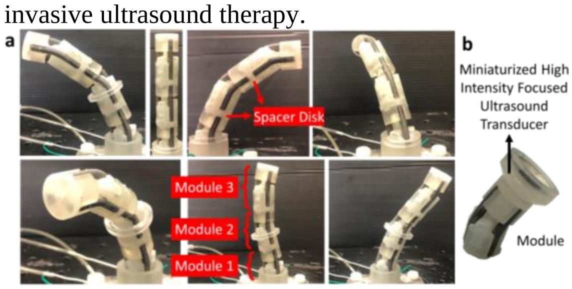

Fig. 4 Modular manipulator by integrating three modules in various configurations.

REFERENCES

[1] S. S. R. Chennareddy, A. Agrawal, and A. Karuppiah, 'Modular Self-Reconfigurable Robotic Systems: A Survey on Hardware Architectures', *J. Robot.*, vol. 2017, pp. 1–19, 2017.

[2] C. Zhang, P. Zhu, Y. Lin, Z. Jiao, and J. Zou, 'Modular Soft Robotics: Modular Units, Connection Mechanisms, and Applications', *Adv. Intell. Syst.*, vol. 2, no. 6, p. 1900166, Jun. 2020.

[3] A. Arezzo *et al.*, 'Total mesorectal excision using a soft and flexible robotic arm: a feasibility study in cadaver models', *Surg. Endosc.*, vol. 31, no. 1, pp. 264–273, Jan. 2017.

[4] B. T. Phillips *et al.*, 'A Dexterous, Glove-Based Teleoperable Low-Power Soft Robotic Arm for Delicate Deep-Sea Biological Exploration', *Sci. Rep.*, vol. 8, no. 1, p. 14779, Dec. 2018.

[5] C. Sozer, L. Paternò, G. Tortora, and A. Menciassi, 'A Novel Pressure-Controlled Revolute Joint with Variable Stiffness', *Soft Robot.*, p. soro.2020.0196, Jul. 2021.